Diabetologia

Identification of a single nucleotide polymorphism showing no insulin-mediated suppression of the promoter activity in the human insulin receptor substrate 2 gene

K. Iwamoto, H. Mori, H. Okazawa, M. Hashiramoto, M. Kasuga

Division of Diabetes, Digestive and Kidney Diseases, Department of Clinical Molecular Medicine, Kobe University, Japan

Abstract

Aims/hypothesis. To understand the transcriptional regulation and to investigate the pathological influence upon Type II (non-insulin-dependent) diabetes mellitus of insulin receptor substrate 2 (*IRS2*), the 5′ flanking region of the human *IRS2* gene was cloned and screened in Japanese diabetic patients.
Methods. Luciferase reporter assay and electrophoretic mobility shift assay (EMSA) were combined in HepG2, Fao, RINm5F, and HeLa cells to characterise the human *IRS2* promoter region. Single nucleotide polymorphisms (SNPs) were identified in Japanese Type II diabetic patients by sequencing and were genotyped.
Results. The proximal 2399 bp of the 5′ flanking region of the human *IRS2* gene was cloned. A core promoter region was extended between nucleotide positions –834 and –557 (relative to the translation initiation site). The region [(–758)AGGGGGAGGG(–749)] that appears important in the positive regulation of

IRS2 transcription was identified by EMSA with ^{32}P-labelled double-stranded oligonucleotides encompassing regions protected from DNase I digestion by nuclear extract of HepG2 cells. Two SNPs (–765*C/T* and –2062*T/C*), identified by screening Japanese Type II diabetic patients, were not associated with Type II diabetes. *IRS2*-driven reporter activity in the plasmid containing thymine at –765 was not suppressed by insulin when measured in Fao cells.
Conclusion/interpretation. The 5′ flanking sequence of the human *IRS2* was investigated and two SNPs were identified. The SNP at –765 was suggested to be involved in the insulin-mediated regulation of the transcriptional activity of *IRS2*. [Diabetologia (2002) 45:1182–1195]

Keywords Insulin receptor substrate 2, promoter, transcription, luciferase assay, insulin, Fao, insulin-responsive element, Type II diabetes, genetics, single nucleotide polymorphism.

Corresponding author: M. Hashiramoto, MD, PhD, Division of Diabetes, Digestive and Kidney Diseases, Department of Clinical Molecular Medicine, Kobe University Graduate School of Medicine, 7-5-1 Kusunoki-Cho, Chuo-Ku, Kobe 650-0017, Japan. E-mail: hashira@med.kobe-u.ac.jp
Abbreviations: IRS, Insulin receptor substrate; IR, insulin receptor; PI3K, phosphatidylinositol 3-kinase; DM, diabetes mellitus; nt, nucleotide; PCR, polymerase chain reaction; DTT, dithiothreitol; EMSA, electrophoretic mobility-shift analysis; UV, ultraviolet; PAGE, polyacrylamide gel electrophoresis; C/EBP CCAAT, enhancer binding protein; HNF3, hepatocyte nuclear factor 3; MZF1, myeloid zinc finger protein 1; HSF, heat shock factor; GKLF, gut Krüppel-like factor; RFLP, restriction fragment length polymorphism analysis; SNP, single nucleotide polymorphism; IRE, insulin responsive element; UTR, untranslated region; ANCOVA, analysis of covariance.

The insulin receptor substrate (IRS) proteins are phosphorylated by the insulin receptor (IR) and mediate the actions of insulin by acting as adapter or scaffolding molecules [1]. To date, four IRS proteins (IRS1 to IRS4) have been identified, all of which possess a conserved domain structure that includes pleckstrin homology and phosphotyrosine-binding domains in the NH_2-terminal region [2, 3, 4, 5, 6]. The COOH-terminal region of these proteins is poorly conserved, with the exception of the presence of multiple motifs that undergo tyrosine phosphorylation in response to insulin and serve as docking sites for Src homology 2 domain-containing proteins, such as phosphatidylinositol 3-kinase (PI3K), SH2 domain-containing phosphotyrosine phosphatase (SHP2), and Grb2. These motifs are therefore thought to mediate most IR downstream signalling events that cause insulin action.

IRS1 mediates several cellular responses to insulin stimulation, including mitogenesis, protein synthesis, and glucose transport [1]. Mice deficient in IRS1 show marked growth retardation, mild insulin resistance with normal basal glucose concentrations and fasting hyperinsulinaemia, and an increased beta-cell mass [7, 8, 9, 10] but they do not develop diabetes. In addition, although variants of the human *IRS1* gene have been detected, these mutations account for disease in only a small proportion of patients with Type II (non-insulin-dependent) diabetes mellitus [11, 12].

IRS2 was initially discovered as an interleukin-4 receptor substrate and was subsequently shown to be an IRS that was phosphorylated in cells from IRS1-deficient mice [13]. It has been suggested that insulin resistance induced by IRS1 deficiency can be compensated for by *IRS2* and increased insulin production, thereby explaining the non-diabetic phenotype of IRS1 knockout mice [1]. Homozygous disruption of the *IRS2* gene in mice results in progressive deterioration of glucose homeostasis, characterised by an increase in fasting hyperglycaemia, and overt diabetes [9]. Morphometric analysis of the pancreatic islets of these mice showed a marked reduction in beta-cell mass, which prevents an increase in the concentration of insulin secretion sufficient to compensate for the insulin resistance. These observations suggested that functional defects in *IRS2* could contribute to Type II diabetes by impairing insulin production (through effects on beta-cell neogenesis, proliferation, or survival) and insulin action.

Nucleotide substitutions have been detected in the coding region of the human *IRS2* gene [14, 15, 16]. Among them, only the Gly^{1057} → Asp is predicted to contribute to the prevalence of Type II diabetes mellitus since Asp^{1057} carriers can have higher insulin sensitivity [16]. Given that genetic variability in promoter sequences potentially affects the level of protein expression, the organisation and 5′ flanking sequence of human *IRS2* were recently examined [15, 17, 18]. However, the promoter sequence described was only partial and the genetic variability of this sequence in diabetic subjects was not intensively investigated.

We therefore designed our studies to sequence and characterise the 5′ untranslated region (UTR) of the human *IRS2* gene and to screen this region for mutations in Japanese diabetic patients. We also investigated the potential mechanism for the insulin-mediated repression of the *IRS2* gene by using the polymorphisms which were identified.

Subjects and methods

Cloning of the human IRS2 gene. Two DNA fragments encompassing the protein-coding region of human *IRS2* [nucleotides (nt) 73 to 395 and 3537 to 3992] were obtained by polymerase chain reaction (PCR) amplification with a human placental genomic DNA library (Clontech, Palo Alto, Calif., USA) as template and two pairs of primers [5′-aacaacaacaaccacagcgtc-3′ (forward) and 5′-tcctgctcctgctcgttcctc-3′ (reverse); 5′-tgtctct-ctcaggaaaagcag-3′ (forward) and 5′-ttcaagtggtgggacaagaag-3′ (reverse), respectively, based on the gene sequence in Gene-Bank (accession no. AB000732)]. These fragments were then used as probes to screen the same genomic library for human *IRS2*. Three clones that initially tested positive with both probes were confirmed to be derived from human *IRS2* by Southern blot analysis, and were subcloned into the pBlue-script II KS(+) vector (Stratagene, La Jolla, Calif., USA) and sequenced with an ABI PRISM 377 DNA sequencing system (Perkin Elmer, Norwalk, Conn., USA). Transcription factor binding sites were analysed with Transcription Factor Search (TFSEARCH) [19, 20].

Generation of luciferase reporter constructs. The transcriptional activity of the human *IRS2* promoter was analysed with the use of the promoterless luciferase expression plasmid pGL3-Basic (Promega, Madison, Wis., USA). A 2.6-kb fragment of the promoter (nt –2399 to +217) was isolated from human *IRS2* by digestion with XhoI and inserted into the XhoI site of pBluescript II KS(+), thereby generating pBS-5′hIRS2. An initial series of deletion constructs corresponding to specific portions of the cloned 5′ UTR was generated with the use of available restriction sites and subcloning into equivalent sites. The largest fragment of the promoter sequence (nt –2399 to –124) was obtained by digestion of pBS-5′hIRS2 with SacI [site located in the multiple cloning region of pBluescript II KS(+), upstream from the *IRS2* sequence] and MluI (site located at nt –124 of *IRS2*), and was subcloned into the corresponding sites of pGL3-Basic. The resultant plasmid, which contained the promoter in the correct orientation, was designated pGL3-IRS2(–2399).

To generate pGL3-IRS2(–1824), we first subcloned an ~2- kb EcoRI-XhoI fragment of the promoter (–1824 to +217) into the EcoRI and XhoI sites of pBluescript II KS(+); the SacI-MluI fragment of the resulting construct was then excised and ligated into the SacI and MluI sites of pGL3-Basic. To construct pGL3-IRS2(–2116), we amplified ~300-bp DNA fragments by PCR with pBS-5′hIRS2 as template, a forward primer (5′-TTCTATGAATTCTAGAGGACATC-3′), and a reverse primer (5′-TGCTTCGAATTCATGTATCTAC T-3′); the forward primer introduced a mutation that created an EcoRI site that permitted the direct subcloning of this fragment. The resulting PCR product was digested with EcoRI, purified with a QIAquick PCR purification kit (Qiagen, Valencia, Calif., USA), and subcloned into the EcoRI site of pGL3-IRS2 (–1824).

For the construction of pGL3-IRS2(–1572) and pGL3-IRS2(–269), pBS-5′hIRS2 was digested with PstI [sites located in the multiple cloning region of pBluescript II KS(+), upstream of the *IRS2* promoter, and at nt –1572 of *IRS2*] or NotI [sites located in the multiple cloning region of pBluescript II KS(+), upstream of the *IRS2* sequence, and at nt –269 of *IRS2*] to remove the 5′ flanking sequence upstream of nt –1572 and –269, respectively. The remaining sequences were self-ligated and then digested with SacI and MluI and the resulting fragments were inserted into the SacI-MluI sites of pGL3-Basic.

The constructs pGL3-IRS2(–1232), pGL3-IRS2(–834), and pGL3-IRS2(–556) were generated by digestion of pBS-5′hIRS2 with EcoRV [site located in the multiple cloning region of pBluescript II KS(+), upstream from the *IRS2* promoter] and either NruI, NaeI, or SapI (sites located within the *IRS2* sequence), respectively. The remaining sequences were self-ligated and then digested with SacI and MluI and the resulting fragments were ligated into SacI-digested and MluI-digested pGL3-Basic.

A second series of deletion constructs was generated by PCR amplification of DNA fragments spanning nt –786, –743, –674, –635, or –600 to –124 with pGL3-IRS2(–1232) as template, five different forward primers (5′-CCCGAGCTCGC-CCGGC-3′, 5′-GAGGGGAGCTCGGGAAAC-3′, 5′-AGCG-GAGCTCCGATTGGC-3′, 5′-GGCGGAGCTCCAATGCG-3′, and 5′-GGCCGAGCTCTGTGTGC-3′, respectively), and a common reverse primer (5′-CCCGATCACGCGTCCCT-3′); each of the forward primers introduced a mutation to create a SacI site that facilitated the subcloning of these fragments. The resultant PCR products were digested with SacI and MluI, purified with a QIAquick PCR purification kit, and ligated into the corresponding sites of pGL3-Basic, yielding the plasmids pGL3-IRS2(–786), pGL3-IRS2(–743), pGL3-IRS2 (–674), pGL3-IRS2(–635), and pGL3-IRS2(–600), respectively.

In vitro mutagenesis was done with a Quikchange Site-Directed Mutagenesis Kit (Stratagene), the pGL3-IRS2(–834) plasmid as template, and the following oligonucleotides (mutated sequences underlined) that disrupted protein binding at specific sites in the identified footprint regions: footprint 1, GGCCTCCGCGGAAAGGGGAAAGGACGGCGGGAAAC; footprint 2, GGGGAGAAAGGGGTTCGGTTCGGGTTCGC-GCGGCCCGCCC, an insulin responsive element (IRE): CGCCGAGTCACATGTTGCCTTGCTCTTCTTAG, and an identified SNP at nt –765 of *IRS2*, substituting C to T: CGGGCCGGGGCCTTCGCGGGAGGGGGA. The latter two plasmids generated were designated pGL3-IRS2-mutIRE and pGL3-IRS2(-765T), respectively. The orientation and sequence of all constructs were verified by direct sequencing.

Transient transfection of cultured cells and assay of luciferase activity. Plasmids used for transfection were purified with a Qiagen plasmid kit after phenol-chloroform precipitation. HepG2, Fao, RINm5F and HeLa (RIKEN, Tsukuba, Japan) cells were grown under an atmosphere of 5% CO_2 at 37°C in DMEM supplemented with 10% foetal bovine serum, 2 mmol/l L-glutamate, penicillin (100 U/l), and streptomycin (100 mg/l). The day before transfection, cells were transferred to six-well culture dishes at a density that ensured that they would achieve 70 to 80% confluence by the time of transfection. Cells were transfected with 1 µg of luciferase reporter construct DNA and 100 ng of the internal control plasmid pRL-TK (Promega) with the use of FUGENE 6 (Roche, Indianapolis, Ind., USA). For the experiments in Fig. 7, the medium was replaced with serum-free DMEM 8 h after transfection and incubated for 16 h to establish a basal condition followed by additional incubation in the absence or presence of 10^{-7} mol/l insulin for 16 h. At 40 h after transfection, the culture medium was removed and the cells were washed with a phosphate-buffered saline solution [137 mmol/l NaCl, 2.7 mmol/l KCl, 1.5 mmol/l KH_2PO_4, 8.0 mmol/L Na_2HPO_4 (pH 7.4)]. Lysis buffer (500 µl) provided with the Dual-Luciferase Reporter Assay System (Promega) was added to each well and the culture plates were gently agitated for 30 min at room temperature. The cell lysates were then transferred to microfuge tubes and centrifuged at 12 000×g for 3 min, after which the resulting supernatants were assayed sequentially for firefly and Renilla luciferase activities with the Dual-Luciferase Reporter Assay System (Promega) and a 1253 Luminometer (Bio-Orbit, Turku, Finland). The activity of Renilla luciferase, expressed from the pRL-TK plasmid under the control of the thymidine kinase promoter, provided an internal control to monitor transfection efficiency. The firefly luciferase activity was thus normalised on the basis of Renilla luciferase activity.

Preparation of nuclear extracts. Nuclear extracts were prepared from HepG2 or Fao cells as described [21] with minor modifications. In brief, cells were rinsed with and scraped into phosphate-buffered saline and then isolated by centrifugation at 1500×g for 5 min. The resulting pellet was resuspended in a solution containing 10 mmol/l HEPES-KOH (pH 7.9), 10 mmol/l KCl, 0.1 mmol/l EDTA, 0.1 mmol/l EGTA, 1 mmol/l dithiothreitol (DTT) and 0.5 mmol/l phenylmethylsulfonyl fluoride. Nonidet P-40 (Nacalitesque, Kyoto, Japan) was then added to the cells on ice to a final concentration of 0.5%, and the tube was mixed vigorously for 30 s. The nuclei were separated by centrifugation and extracted with a solution containing 50 mmol/l HEPES-KOH (pH 7.9), 420 mmol/l KCl, 5 mmol/l $MgCl_2$, 0.1 mmol/l EDTA, 1 mmol/l DTT, 20% glycerol and 0.5 mmol/l phenylmethylsulfonyl fluoride. The concentration of the nuclear extract was measured with a protein assay reagent (BioRad, Hercules, Calif., USA).

DNase I footprint analysis. A DNA fragment (nt –1102 to –611) was obtained by digesting pGL3-IRS2(-1232) with NotI and treated with calf intestinal alkaline phosphatase (TAKARA, Otsu, Japan). The released oligonucleotide was isolated by gel electrophoresis and 5′-end-labelled with the use of T4 polynucleotide kinase (TAKARA) and [γ-^{32}P]ATP (ICN, Costa Mesa, Calif., USA). The labelled DNA was digested with ApaI to remove the 196-bp DNA from the distal end of the *IRS2* promoter sequence. The resulting DNA fragment thus labelled only at the proximal end (corresponding to nt –906 to –611 of *IRS2*) was gel-extracted and purified with the use of a QIAGEN Kit (Qiagen).

The purified double-stranded probe (10 ng, ~30 000 cpm) was incubated at room temperature for 30 min with 30 µg of HepG2 nuclear extract in a volume of 50 µl containing 4 µg of poly(dI-dC)·poly(dI-dC) (Amersham Pharmacia Biotech, Little Chalfont, UK), 1.25 µg of salmon testis DNA, 10 mmol/l HEPES-KOH (pH 7.9), 80 mmol/l KCl, 5 mmol/l $MgCl_2$, 1 mmol/l EDTA, 0.5 mmol/l DTT, and 4% glycerol. After adding 5 µl of a solution containing 5 mmol/l $CaCl_2$ and 10 mmol/l $MgCl_2$, the mixture was incubated for an additional 1 min at room temperature. DNase I (0.35 U) (Amersham Pharmacia Biotech) was then added to the reaction mixture and incubation was continued for an additional 1 min at room temperature. The reaction was terminated by adding 140 µl of a solution containing 190 mmol/l sodium acetate, 30 mmol/l EDTA, 0.14% SDS, and yeast tRNA (64 µg/ml). After the addition of 5 U of proteinase K (Wako, Osaka, Japan) and incubation for 30 min at 50°C, the DNase I-digested DNA was purified by phenol-chloroform extraction and ethanol precipitation and then subjected to electrophoresis on a 6% polyacrylamide gel containing 8 mol/l urea. A G+A sequencing ladder was generated by removing modified bases of the probe with 4% formic acid and subsequent cleavage with piperidine at G and A residues.

Electrophoretic mobility-shift assay (EMSA) analysis. Oligonucleotides including the sequences for footprint 1 [(–773)CG-GGGCCTCCGCGGGAGGGGGAGGGGACGGCGGGAAA-CG(–735)], footprint 2 [(–726)GGAGAAAGGGGGGCGGGG-CGGGGGC(–702)], –765C [(–777) CGGGCCGGGGCCTCC-GCGGGAGGGGGA (–751)] and –765T [(–777) CGGGCC-GGGGCCTTCGCGGGAGGGGGA (–751)] of the *IRS2* promoter were synthesised in both sense and antisense strands as single-stranded molecules, the corresponding pairs of which were first incubated at 85°C for 5 min in annealing buffer [20 mmol/l Tris-HCl (pH 7.5), 10 mmol/l $MgCl_2$, 50 mmol/l NaCl] and then gradually cooled to 45°C to generate double-stranded DNA molecules. The double-stranded molecules were labelled with [γ-^{32}P]ATP and used as probes in EMSA experiments. HepG2 and Fao nuclear extract (5 µg of protein) was

incubated for 30 min at room temperature with 1 µg of poly(dI-dC)·poly(dI-dC) and 0.1 µg of salmon testis DNA in a total volume of 20 µl containing 10 mmol/l HEPES-KOH (pH 7.9), 50 mmol/l KCl, 5 mmol/l MgCl$_2$, 1 mmol/l EDTA, 0.5 mmol/l DTT, and 5% glycerol. After the addition of 1 µl (0.8 ng, ~25,000 cpm) of ^{32}P-labelled probe, the mixture was incubated for an additional 30 min at room temperature.

For experiments in Fig. 4B, mutant oligonucleotides (mutated sequences are underlined) were synthesised and included in the reaction mixture as follows. For analysis of the footprint 1 region: 1–1, AAAAACCTCCGCGGGGAGGGGGGAGGGGA-CGGCGGGAAACG; 1-2, CGGGGAAAAAGCGGGGAGGG-GGAGGGGACGGCGGGAAACG; 1-3, CGGGGCCTCCAA-AAAAGGGGGGAGGGGACGGCGGGAAACG; 1-4, CGGG-GCCTCCGCGGGAAAAAGAGGGGACGGCGGGAAACG; 1-5, CGGGGCCTCCGCGGGGAGGGGAAAAAGACGGCGG-GAAACG; 1-6, CGGGGCCTCCGCGGGGAGGGGGGAGGG-AAAAACGGGAAACG; 1-7, CGGGGCCTCCGCGGGGAGG-GGGAGGGGACGGAAAAAAACG; and 1-8, CGGGGCCT-CCGCGGGGAGGGGGGAGGGGACGGCGGGAAAAA.

For supershift experiments, the indicated antibodies (1 to 3 µg) were added to the reaction mixture before the incubation with labelled probe, and the resulting mixture was then incubated for an additional 30 min at room temperature. Polyclonal antibodies to Sp1, Sp2, Sp3, Sp4, GKLF, HSF-1, AP2α, or E2F-1 were obtained from Santa Cruz Biotechnology (Santa Cruz, Calif., USA). All reaction mixtures were finally fractionated by electrophoresis on a nondenaturing 5% polyacrylamide gel, which was then dried and subjected to autoradiography with Kodak Biomax MS film.

Ultraviolet (UV)-induced cross-linking. A 22-nucleotide double-stranded oligomer based on the sequence of the footprint 1 region and its mutated derivatives were prepared and labelled as described above for EMSA experiments. The sequences (5′→3′) of these oligonucleotides were as follows (mutated sequences underlined): the wild-type probe, (–765)CCGCGG-GAGGGGGGAGGGGACGG(–744); dual-mutant probe, CCG-CGGAAAGGGGGAAAGGACGG; front-mutant probe, CCGC-GGAAAGGGGGAGGGGACGG; and rear-mutant, CCGCGG-GAGGGGGGAAAGGACGG. Labelled probes were incubated with 10 µg of HepG2 nuclear extract in a volume of 50 µl to allow binding to reach equilibrium, as described above for EMSA analysis. The reaction mixture was then cooled on ice and irradiated for 20 or 60 min at a distance of 5 cm with a UV transilluminator fitted with a 254 nm filter (Funakoshi, Tokyo, Japan). Samples were not treated with nuclease given that the substrate DNAs were labelled at their 5′ ends. Cross-linked complexes were analysed by SDS-polyacrylamide gel electrophoresis (PAGE) on a 10% gel as described [22] and visualised by autoradiography.

Southwestern blot analysis. HepG2 nuclear extract (15 and 60 µg) was subjected to SDS-PAGE on a 10% gel and the separated proteins were transferred electrophoretically to a polyvinylidene difluoride membrane (Millipore, Medford, Mass., USA). The membrane was incubated at room temperature for 30 min in hybridization buffer [10 mmol/l HEPES-KOH (pH 7.9), 50 mmol/l KCl, 5 mmol/l MgCl$_2$, 1 mmol/l EDTA, 0.5 mmol/l DTT, 5% glycerol] containing 5% non-fat dried milk, and then rinsed twice with the same buffer containing 0.25% non-fat dried milk. The membrane was then exposed for 2 h at room temperature to an end-labelled double-stranded oligonucleotide corresponding to either the wild-type or dual-mutant probe (described above for UV cross-linking) in hybridisation buffer containing 0.25% non-fat dried milk. After washing four times with hybridization buffer containing 0.25% non-fat

dried milk, the membrane was dried and subjected to autoradiography.

Patients and control subjects. All study subjects (*n*=549) were Japanese, unrelated and gave their written informed consent to participate in the study for the identification of Type II diabetes genes in Japan [23, 24]. They were 301 patients with Type II diabetes [176 men, 125 women; age, 63.7±10.1 years (mean ± SD); BMI, 23.1±3.3 kg/m^2] and 248 healthy control subjects (114 men, 134 women; age, 75.7±8.5 years; BMI, 21.4±3.7 kg/m^2). The diagnosis of diabetes mellitus was based on the criteria of the World Health Organization [25]. The healthy control subjects were selected according to the following criteria: no past history of urinary sugar or of glucose intolerance, an HbA$_{1c}$ level of less than 5.6%, an age of older than 60 years, and no family history of diabetes mellitus. These criteria which could enhance statistical power to detect associations were also used in previous reports from our laboratory [23, 24]. The investigation was carried out in accordance with the guidelines expressed in the Declaration of Helsinki.

Clinical assessment. The sex and present age were ascertained from medical records. Present BMI were directly measured when we collected blood samples to obtain DNA. The fasting plasma concentration of glucose (FPG), the fasting plasma concentration of immunoreactive insulin (f-IRI), and the HbA$_{1c}$ level were measured by standard laboratory techniques. Based on the assumption that control subjects younger than 35 years and of normal weight exhibit 100% beta-cell function and an insulin resistance of 1, the corresponding values for those with diabetes can be assessed from FPG and f-IRI by the following formulas: homeostasis model assessment for beta-cell function (HOMA-β, expressed as a percentage) = f-IRI×20/(FPG–3.5), and homeostasis model assessment for insulin resistance (HOMA-R, expressed in mol µU l$^{–2}$) = FPG×f-IRI/22.5 [26].

Screening and genotype analysis of the single nucleotide polymorphisms (SNPs). Genomic DNA was isolated from the peripheral blood leukocytes of all study participants and subjected to PCR-based direct sequence to screen 25 diabetic patients for mutations in the 5′ flanking region of human *IRS2*. PCR-based direct sequence was also carried out to assess the genotypes with regard to the detected –765*C/T* polymorphism. Fragments of *IRS2* encompassing the polymorphic site (–765*C/T*) were amplified by PCR with the sense primer 5′-CCACAACA-AGCCGCTGATTAT-3′ and the antisense primer 5′-TTGCTG-CTGCTGCTGCCAAC-3′, and subjected to direct sequencing analysis. For –2062 *T/C* polymorphism, PCR and restriction fragment length polymorphism analysis (PCR-RFLP) was done to evaluate its allele frequencies. Fragments of the human *IRS2* encompassing the polymorphic site (-2062 *T/C*) were amplified by PCR with the sense primer 5′-CTAACTGTATACATGCT-AAAAAT-3′ and the antisense primer 5′-AACAAAACAGG-CTTT-3′. The resulting PCR product obtained from subjects with the T allele contains a Ssp I restriction site but not with the C allele. The 334- bp PCR products of *IRS2* were therefore digested with Ssp I, subjected to electrophoresis on a 12% polyacrylamide gel, and visualised by staining with ethidium bromide. The genotype of each study subject was determined blindly, without knowledge of clinical status.

Statistical analysis. All data are presented as means ± SD or proportions. The allele frequencies for SNPs between Type II diabetic and control groups were compared by a standard chi-square test. Other categorical variables were also compared by the chi-square test. An estimation of linkage disequilibrium

between the detected two SNPs was done by using the Estimating Haplotype (EH) frequencies version 1.11 software program (ftp://linkage.rockefeller.edu/software/eh). Comparison of quantitative variables was done using ANOVA. The effect of genotype on the clinical parameters was estimated by analysis of covariance (ANCOVA) using genotype as a factor and age and sex as covariates. Statistical analyses except the estimation of linkage disequilibrium was done with Stat View Version 5.0 (SAS Institute, Cary, N.C., USA). A p value of less than 0.01 was considered to be significant in the context of multiple testing.

Results

Cloning and sequencing of the 5′ flanking region of the human IRS2 gene. We isolated three human *IRS2* clones by screening a genomic DNA library with two specific probes (Fig. 1A). All three clones reacted with both probes in Southern blot analysis and were subjected to partial sequencing, the results of which suggested that they contain most of the protein-coding region of *IRS2*. The results of Southern blot analysis, nucleotide sequencing, and restriction enzyme analysis showed that partial nucleotide sequences of clone 1 and clone 3 were consistent with each other and clone 1 contained the longest 5′ flanking sequence (~2.4 kb) of the three clones. We thus selected clone 1 for further analysis.

The nucleotide sequence of clone 1 (nt –2399 to +217, relative to the translation start site) is shown in Fig. 1B. A TATA box is located at nt –2190 to –2184. Analysis of transcription factor binding sites with TFSEARCH located several putative binding motifs for various transcription factors in the 5′ flanking region of human *IRS2* (Fig. 1A).

Activity of the IRS2 promoter in various cell types. To identify the portions of the 5′ flanking region of *IRS2* required for maximal promoter activity, a series of 5′ deletion mutants, constructed into the promoterless luciferase expression plasmid pGL3-Basic, were introduced into HepG2, Fao, RINm5F, and HeLa cells. We used these cell lines because *IRS2* is abundantly expressed in liver and was suggested to be involved in the beta-cell proliferation. The promoter activity of

each deletion mutant was then evaluated by assay of luciferase activity in extracts of the transfected cells.

Deletion analysis in HepG2 cells showed that truncation of the 5′ upstream sequence from nt –2399 [pGL3-IRS2(–2399)] to nt –834 [pGL3-IRS2(–834)] had no marked effect on the transcriptional activity of the human *IRS2* promoter. Further deletion to position
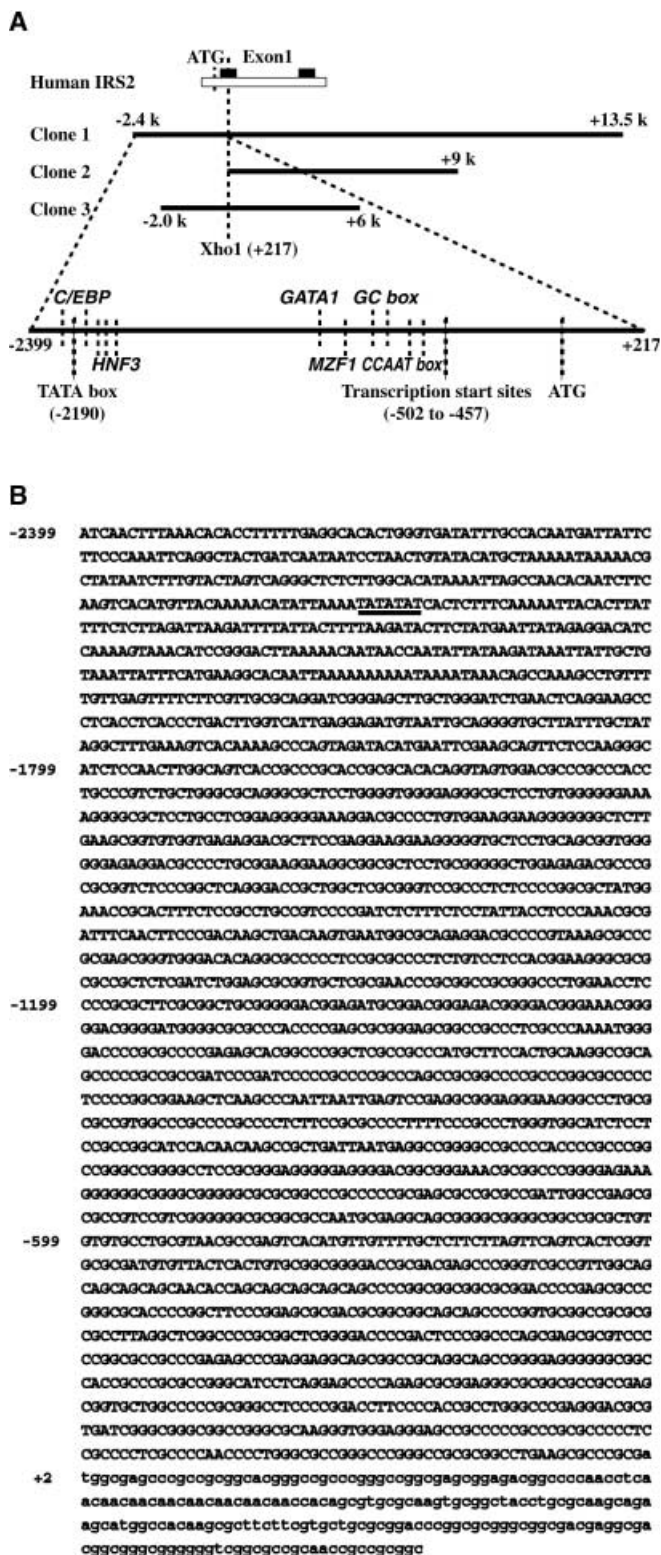

Fig. 1A,B. Structural organisation and nucleotide sequence of the promoter region of human *IRS2*. **A** Structural organisation of the 5′ flanking region of human *IRS2*. The *small filled boxes* above the representation of the gene correspond to the probes used to screen the human genomic DNA library. The positions of the three genomic DNA fragments (clones 1, 2, and 3) isolated from this library are also indicated. The locations of a TATA box, the predicted transcription initiation site, the translation initiation codon (ATG), and putative transcription factor binding sites are shown in the *lower schematic*. **B** Nucleotide sequence of the promoter region of human *IRS2*. The 5′ flanking sequence is shown in *uppercase letters* and the coding sequence in *lowercase letters*. The underlined sequence indicates the TATA element. All positions are numbered relative to the A of the translation start codon (ATG) as position +1. (The human *IRS2* promoter sequence has been deposited in DDBJ/EMBL/GenBank under the accession number AB050954)
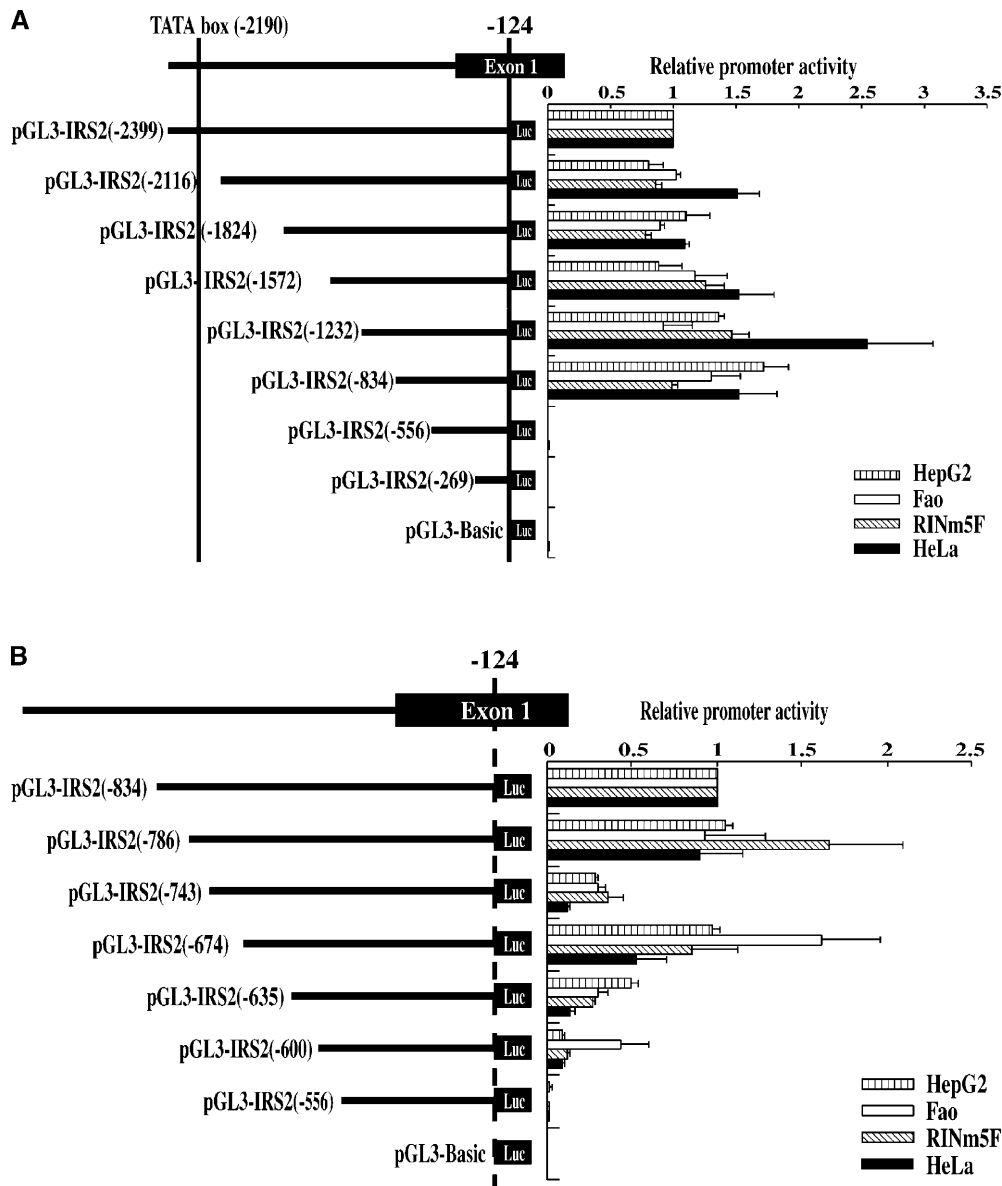
Fig. 2A,B. Effects of deletion of the human *IRS2* promoter on transcriptional activity. The 2.4-kb 5′ flanking region of *IRS2* and its deletion mutants are shown in the *left panels*. The promoter fragments, terminating at nt –124 and beginning at the indicated positions between –2399 and –269, were inserted into pGL3-Basic, and the resulting constructs were introduced into HepG2, Fao, RINm5F or HeLa cells. Normalised firefly luciferase activity of cell lysates is shown in the *right panels* and is expressed as a percentage of that apparent in cells transfected either with pGL3-IRS2(–2399) (**A**) or with pGL3-IRS2(–834) (**B**). Data are means ± SE of values from three to six experiments and two independent transfections

–556, however, reduced the promoter activity to about 0.5% of that apparent with pGL3-IRS2(–2399) (Fig. 2A). Similar results were observed when these deletion constructs were transfected in other three cell lines (Fig. 2A). These data indicated that the core promoter of human *IRS2* is located within the 278- bp region between nt –834 and –557.

To delineate more precisely the transcriptional regulatory elements within the core promoter of *IRS2* spanning nt –834 to –556, we prepared an additional series of deletion mutants and measured their transcriptional activities in four different cell lines (Fig. 2B). Compared with the activity of the pGL3-IRS2(–834) construct, deletion to position –786 [pGL3-IRS2(–786)] did not affect promoter activity whereas deletion to position –743 [pGL3-IRS2(–743)] resulted in approximately a 70% decrease in activity. Further deletion to position –674 restored the promoter activity to between 50 and 100% of that of pGL3-IRS2(–834), whereas progressive deletions from nt –674 to nt –556 resulted again in a gradual decrease in activity. These results indicated that sequences located between positions –786 and –744 and between positions –674 and –557 positively regulate *IRS2* promoter activity, whereas a sequence between positions –743 and –675 negatively regulates the promoter activity.
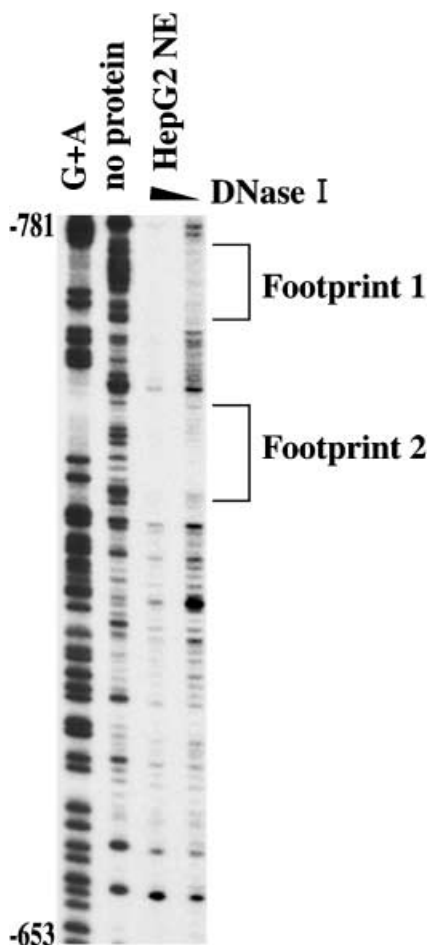
Fig. 3. DNase I footprint analysis of the *IRS2* core promoter region. A double-stranded DNA probe corresponding to nt –904 to –611 of human *IRS2* and end-labelled with ^{32}P was incubated in the absence or presence of 30 µg of HepG2 nuclear extract (NE) and subsequently digested with decreasing amount of DNase I. Sequence analysis of the antisense DNA strand is shown, with numbers corresponding to nucleotide positions. Two regions protected from DNase I digestion by the nuclear extract are designated footprints 1 and 2. Lane G+A, G+A sequencing ladder of the probe. Data are representative of six similar experiments

DNase I footprint analysis of the IRS2 gene promoter. To locate the sequence of *IRS2* in which regulatory proteins potentially bind to the core promoter region of *IRS2* identified by deletion analysis, we did a DNase I footprint analysis with a crude nuclear extract of human hepatoma HepG2 cells and a DNA probe corresponding to nt –904 to –611 of *IRS2*. Two footprints of 39 and 25 bp were identified: footprint 1, nt –773 to –735, and footprint 2, nt –726 to –702, respectively (Fig. 3). Similar results were obtained when we used a different DNA probe corresponding to nt –878 to –512 of *IRS2*.

Analysis of the DNA sequences of footprint 1 and footprint 2 showed the presence of binding motifs in both footprints for various transcription factors, including those for ADR1 and heat shock factor (HSF) as well as GC boxes. In addition, activator protein 2

(AP2), E2 promoter binding factor (E2F), and MZF1 binding sites were detected in footprint 1.

EMSA analysis. To corroborate the results of the DNase I footprint analysis and to identify DNA-binding proteins that interact with the *IRS2* promoter, we prepared a synthetic oligonucleotide encompassing footprint 1 (nt –773 to –735) and subjected it to EMSA analysis with HepG2 nuclear extract.

Incubation of the ^{32}P-labelled probe with HepG2 nuclear extract resulted in the appearance of three major shifted bands (Fig. 4A, arrows) that were not detected in the presence of excess unlabelled probe. Unlabelled oligonucleotides that contained a GC box or the consensus binding sites for AP2, E2F, HSF, ADR1, or MZF1 did not compete with the ^{32}P-labelled probe in its interactions with extract proteins. Supershift analysis showed that polyclonal antibodies to Sp2 or to Sp3 reduced the mobility of the protein-DNA complexes formed by the footprint 1 probe (Fig. 4A, arrowheads).

To identify the nucleotide sequence(s) within footprint1 region that are responsible for the formation of observed DNA-protein complexes, we examined the effects of eight mutant oligonucleotides (footprint 1–1 to 1–8) containing sequential disruptions in the footprint 1 sequence on the formation of DNA-protein complexes by the ^{32}P-labelled footprint 1 probe. Whereas excess footprint 1–4 and footprint 1–5 oligonucleotides had virtually no effect on the DNA-protein complexes formed by the footprint 1 probe, each of the other six mutant oligonucleotides efficiently competed with the footprint 1 probe in the formation of these complexes (Fig. 4B). These results, together with the findings obtained by luciferase assays (Fig. 2), indicated that the sequences mutated in the footprint 1–4 and 1–5 oligonucleotides (nt –758 to –749) positively regulate the transcriptional activity of the *IRS2* promoter by binding unknown nuclear proteins. It was also showed that the consensus binding motifs for either Sp2 or Sp3 were not identical with the identified cis regulatory element (nt –758 to –749).

We also examined by EMSA analysis to identify DNA-binding proteins that interact with the footprint 2 (nt –726 to –702). Incubation of the ^{32}P-labelled probe corresponding to footprint 2 with HepG2 nuclear extract resulted in the appearance of one major and two minor shifted bands that were not detected in the presence of excess unlabelled probe (lane 2 in Fig. 4C). An excess of unlabelled oligonucleotides containing a consensus GC box slightly reduced the intensity of the two minor bands. Consistent with this effect, given that Sp proteins interact with the GC box, supershift analysis showed that polyclonal antibodies to Sp2 or to SP3 reduced the mobility of the two minor DNA-protein complexes formed by the footprint2 probe (Fig. 4C). Specifically, the antibodies
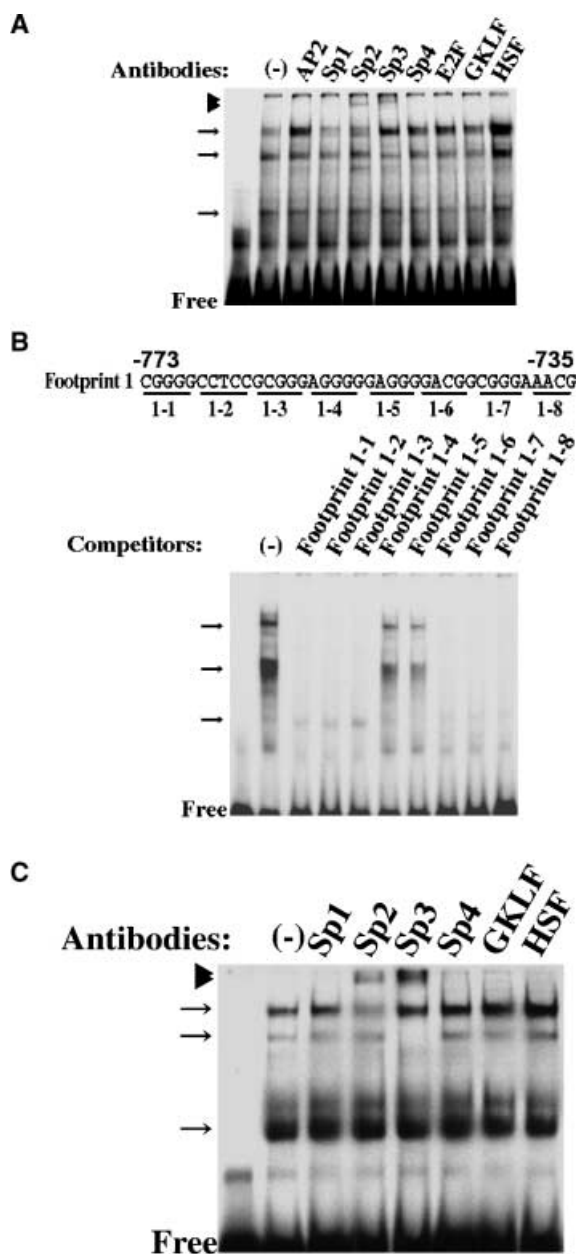
Fig. 4A–C. EMSA analysis with an oligonucleotide corresponding to footprints of the human *IRS2* promoter. EMSA analysis was done with HepG2 nuclear extract (5 µg) and a ³²P-labelled double-stranded oligonucleotide encompassing (**A**, **B**) footprint 1 (nt –773 to –735) and (**C**) footprint 2 (nt –726 to –702) of the *IRS2* promoter. (**A**, **C**) Supershift analysis was done in the presence of antibodies to the indicated proteins. (**B**) Competition analysis was performed in the presence of each of eight oligonucleotides (footprint 1–1 to 1–8) corresponding to the footprint 1 sequence in which the underlined nucleotides were replaced by an equivalent number of A residues. In lane 1 of all panels, the ³²P-labelled footprint 1 probe was applied to the gel without prior incubation with nuclear extract. Shifted bands are indicated with *arrows* and supershifted bands with *arrowheads*. Free, free probe. Data are representative of three similar experiments
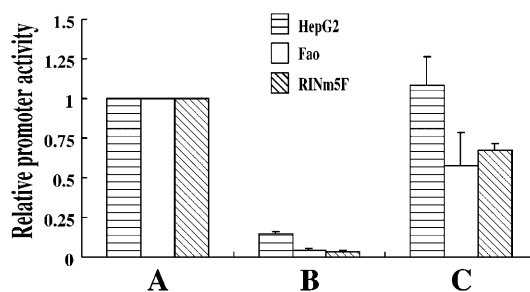

Fig. 5. Effects of point mutations of the human *IRS2* promoter on transcriptional activity. Promoter activity of pGL3-IRS2 (–834) (panel A) and mutations introduced to disrupt potential protein binding sequences in footprints 1 (panel B) and 2 (panel C). The normalised firefly luciferase activity of HepG2, Fao and RINm5F cells transfected with each construct was measured and expressed relative to that of pGL3-IRS2(–834). Data are means ± SE of values from three to six experiments and two independent transfections

to SP3 induced total displacement of one of the shifted bands whereas the antibodies to Sp2 slightly affected both bands. None of the tested antibodies affected the mobility of the major DNA-protein complex formed by the footprint 2 probe. These results suggested that proteins that interact with the GC box play a minor part in the regulation of *IRS2* in this region of the promoter.

Effect of mutation of footprint regions on IRS2 promoter activity. We introduced mutations into pGL3-IRS2(–834) to disrupt the cis regulatory element in footprint 1 (nt –758 to –749) as identified in the above experiment as well as footprint 2 region. The promoter activity of the resulting constructs was assessed in HepG2, Fao, and RINm5F cells. Disruption of the nucleotide sequence in the cis regulatory element in the footprint 1 region resulted in a significant reduction in promoter activity to about 14% in HepG2, 4% in Fao, and 3% in RINm5F cells, respectively, of those apparent with pGL3-IRS2(–834) (Fig. 5A,B). Disruption of GC boxes between positions –715 and –703 of the footprint 2 sequences did not affect promoter activity compared with that of pGL3-IRS2(–834) (Fig. 5C). These results thus largely confirmed the data obtained by EMSA analysis and emphasised the contribution of the cis regulatory element, nt –758 to –749, of footprint 1 in the positive regulation of *IRS2* promoter activity whereas the footprint 2 sequence seemed less important.

UV cross-linking and Southwestern blot analysis of the footprint 1 sequence. To gain further insight into the nature of the proteins that interact with the identified cis regulatory element (nt –758 to –749) in footprint 1, we next carried out UV cross-linking experiments in which the mixtures containing HepG2 nuclear extract and ³²P-Labelled synthetic oligonucleotides encoding the wild-type or mutant cis regulatory ele-
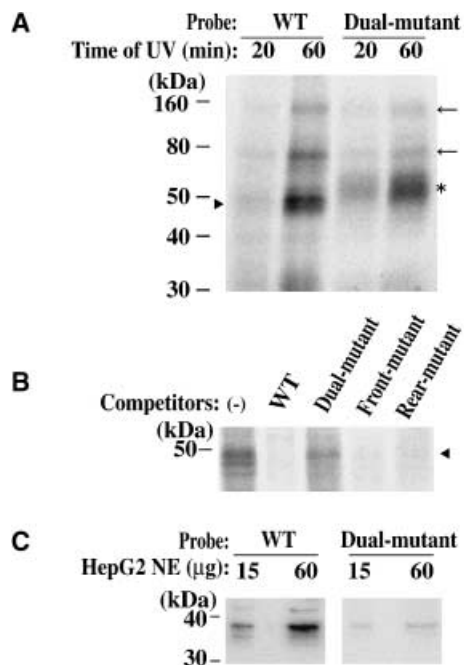
Fig. 6A–C. Characterisation of the protein that interacts with the cis-element of footprint 1 region in the human *IRS2* promoter. **A** UV cross-linking analysis. The cross-linked complexes obtained by incubating either the wild-type (WT) or dual-mutant ^{32}P-Labelled double-stranded oligonucleotides with HepG2 nuclear extract were exposed to UV light for 20 or 60 min and were analysed. The *arrowhead* and *arrows* indicate the major (~50 000 M$_r$) and minor complexes formed, respectively. The *asterisk* indicate the major complex formed only by dual-mutant probe. **B** Competition analysis of UV cross-linking. The ^{32}P-labelled wild-type probe was incubated with nuclear extract in the presence of a 200-fold molar excess of unlabelled wild-type, dual-mutant, front-mutant, or rear-mutant oligonucleotides, after which the reaction mixtures were exposed to UV radiation for 60 min. **C** Southwestern blot analysis. HepG2 nuclear extract (15 or 60 μg) was resolved by SDS-PAGE, and the separated proteins were transferred to a polyvinylidene difluoride membrane and probed with ^{32}P-labelled double-stranded oligonucleotides containing the wild-type (WT) or Dual-mutant probe. DNA-protein complexes were detected by autoradiography. The positions of molecular size markers are indicated in kilodaltons. Data are representative of three similar experiments

Table 1. Genotypes and allele frequencies for the –765*C/T* and the –2062*T/C* polymorphisms in 5′ UTR of *IRS2* for study subjects

	Type II diabetes (n=301)	Control subjects (n=248)
Genotype –765*C/T*		
CC	57	59
CT	161	110
TT	83	79
T allele frequency (%)	54.3[a]	54.0
Genotype –2062*T/C*		
TT	195	164
CT	99	74
CC	7	10
C allele frequency (%)	18.8[b]	18.9

[a] $p=0.924$
[b] $p=0.939$ vs normal control group (chi-square test)
Data are presented in *n* or in %

ment were analysed. The mixtures were then subjected to UV irradiation for 20 or 60 min, and cross-linked DNA-protein complexes were analysed by SDS-PAGE and autoradiography. A major band migrating at a position corresponding to a molecular size of about 50 000 M$_r$ (lane 2, arrowhead in Fig. 6A) and two minor bands at about 75 000 and 150 000 M$_r$ (lane 2, arrows in Fig. 6A) were detected with the wild-type probe. In contrast, the mutant oligonucleotide gave rise to a major band of about 60 000 M$_r$ (lane 4, asterisk in Fig. 6A) and two minor bands at about 75 000 and 150 000 M$_r$ (Fig. 6A, lane 4). These results indicated that the 50 000 M$_r$ complex could contain the protein that binds to the sequence containing the cis-element to increase the transcriptional

activity of the *IRS2* promoter. Competition analysis showed that, whereas oligonucleotides in which nt –759 to –757 or nt –752 to –750 were mutated effectively competed with the ^{32}P-labelled wild-type probe in the formation of the 50 000-M$_r$ complex, a mutant oligonucleotide in which both sequences were disrupted and did not compete (Fig. 6B). These data suggested that both of these sequences are required for the specific binding of the protein contained in the ~50 000 M$_r$ complex. We did a Southwestern blot analysis with HepG2 nuclear extract to evaluate more precisely the molecular size of the protein contained in the ~50 000-M$_r$ complex identified by UV cross-linking, given that this complex also contained the DNA probe. Blot analysis indicated that the size of the major protein that interacts with this sequence is about 37 000 M$_r$ (Fig. 6C), the intensity of which was decreased by the incubation with the dual-mutant probe.

Analysis for genetic variations in the 5′ UTR of the human IRS2. To investigate whether genetic variations contributing to the pathogenesis of Type II diabetes exist within the 5′ UTR of *IRS2*, this region was screened by PCR-based direct sequencing in 25 patients with Type II diabetes. We detected two SNPs: one substituting cytosine (C) to thymine (T) at position –765 (–765*C/T*) and the other replacing T to C at position –2062 (–2062*T/C*). Allele frequencies of the detected two SNPs were evaluated by PCR-based direct sequencing and PCR-RFLP analyses in 301 diabetic patients and 248 control subjects, respectively. The genotypes of both SNPs were in Hardy-Weinberg equilibrium and these two SNPs were in linkage disequilibrium (D=–0.072, $\Delta^2=0.135$, $p=4.27\times10^{-19}$). The allele frequencies for these two SNPs showed no difference between the Type II diabetic group and the control group (Table 1).

Table 2. Characteristics of the study subjects

	Type II diabetes	Control subjects
n (men/women)	301 (176/125)	248 (114/134)
Age (years)	63.7±10.1 (n=301)	75.7±8.5 (n=248)
Age at onset of diabetes (years)	47.0±11.0 (n=295)	
Height (cm)	160±8.9 (n=298)	155±9.0 (n=245)
Weight (kg)	59.0±10.7 (n=298)	51.1±10.2 (n=246)
BMI (kg/m^2)	23.1±3.3 (n=297)	21.4±3.7 (n=245)
Maximum weight (kg)	68.0±11.7 (n=285)	
Age at maximum weight (years)	42.9±13.8 (n=215)	
Maximum BMI (kg/m^2)	26.6±3.6 (n=285)	
Waist-to-hip ratio	0.90±0.08 (n=255)	
HbA_{1c} (%)	7.41±1.40 (n=300)	5.05±0.38 (n=248)
FPG (mg/dl)	139±52 (n=270)	94±15 (n=185)
Fasting IRI (μU/ml)	9.23±10.5 (n=143)	
HOMA-R (mol μU l^{-2})	2.97±2.88 (n=140)	
HOMA-β (%)	48.7±42.6 (n=136)	

Data are presented in means ± SD (n)
FPG, Fasting plasma glucose; IRI, immunoreactive insulin; HOMA-R, homeostasis model assessment for insulin resistance; HOMA-β, homeostasis model assessment for beta-cell function

Table 3. Comparison of clinical profiles for the –765C/T polymorphisms in 5′ UTR of *IRS2* for diabetic patients

	CC	*CT*	*TT*	*p* value[a]
n (men/women)	57 (32/25)	161 (95/66)	83 (49/34)	
Age (years)	64.3±11.8 (n=57)	62.5±9.6 (n=161)	65.4±9.8 (n=83)	0.094
Age at onset of diabetes	46.0±13.0 (n=56)	47.4±10.3 (n=158)	47.4±10.3 (n=81)	0.698
Height (cm)	160±9.5 (n=57)	160±8.9 (n=159)	159±8.6 (n=82)	0.862
Weight (kg)	58.5±10.0 (n=56)	58.8±11.1 (n=159)	59.8±10.5 (n=83)	0.712
BMI (kg/m^2)	23.0±3.1 (n=56)	22.9±3.4 (n=159)	23.4±3.5 (n=82)	0.539
Maximum weight (kg)	68.3±11.5 (n=55)	67.9±12.0 (n=151)	68.1±11.4 (n=79)	0.969
Age at maximum weight (years)	41.4±16.3 (n=37)	41.6±12.6 (n=121)	46.7±14.0 (n=57)	0.051
Maximum BMI (kg/m^2)	26.9±3.5 (n=55)	26.3±3.5 (n=151)	26.9±4.1 (n=79)	0.467
Waist-to-hip ratio	0.90±0.08 (n=50)	0.90±0.08 (n=136)	0.90±0.08 (n=69)	0.884
HbA_{1c} (%)	7.46±1.30 (n=57)	7.43±1.47 (n=160)	7.36±1.37 (n=83)	0.900
FPG (mg/dl)	133±49 (n=49)	138±47 (n=148)	143±63 (n=73)	0.541
Fasting IRI (μU/ml)	11.3± 19.4 (n=29)	8.61±6.46 (n=76)	8.88±6.86 (n=38)	0.486
HOMA-R (mol μU l^{-2})	2.78±2.92 (n=27)	2.93±2.64 (n=76)	3.18±3.37 (n=37)	0.845
HOMA-β (%)	50.6±60.1 (n=26)	50.9±40.4 (n=74)	42.7±31.2 (n=36)	0.620

[a] *p* values were obtained by one-way ANOVA
Data are presented in means ± SD (n)
FPG, Fasting plasma glucose; IRI, immunoreactive insulin; HOMA-R, Homeostasis model assessment for insulin resistance; HOMA-β, Homeostasis model assessment for beta-cell function

The clinical characteristics of the Type II diabetic and control subjects are summarised (Table 2). Among the Type II diabetic patients, no association of genotype for the SNP(–765C/T) with clinical profiles (age, sex, BMI, HbA_{1c}, and fasting plasma glucose) were apparent (Table 3). Significant association of genotype for the SNP(–765C/T) with clinical profiles were neither apparent among the control subjects (Table 4) except that the HbA_{1c} level was lower in subjects bearing T allele(s) at nt –765 (–765C/T or –765T/T) when analysed statistically by ANOVA ([a]*p*=0.003, Table 4) and by ANCOVA using genotype as a factor and age and sex as covariates ([b]*p*=0.006, Table 4). When we compared the clinical profiles in healthy subjects between the SNP(–765C/C) carriers and subjects bearing T allele(s) at nt –765 [SNP(–765C/T) carriers plus SNP(–765T/T) carriers] by two-tailed Student's *t* test, the HbA_{1c} level and fasting plasma glucose concentration were lower in the latter [HbA_{1c}, 5.17±0.31 (n=59) vs 5.01±0.39 (n=189), [a]*p*=0.008; FPG, 99±19 (n=45) vs 92±14 (n=140), *p*=0.011]. Although a gene dosage effect was not evident by having *C* allele at nt –765, these results suggested an adverse role of the minor allele homozygous (CC) in sustaining the lower HbA_{1c} level. Associations of genotype for the SNP(–2062T/C) with clinical profiles were neither significant among the diabetic and control subjects. These results suggested

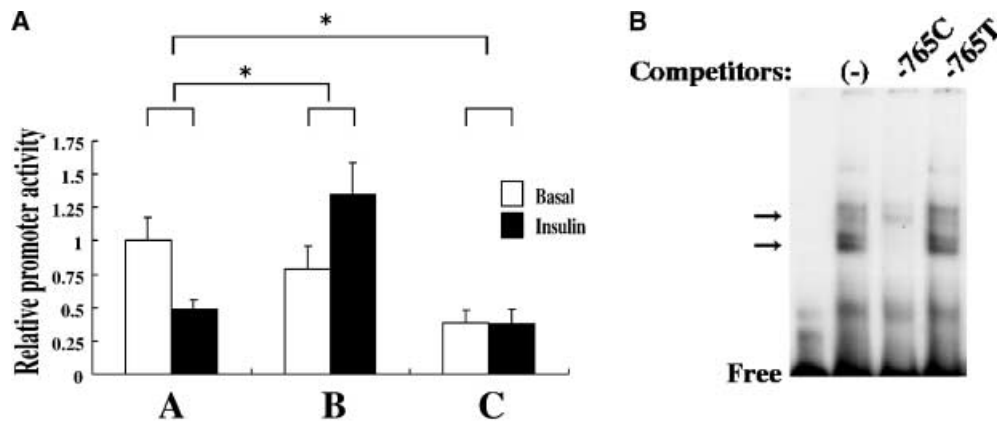**Fig. 7A, B. A** Effect of SNP(–765) and insulin responsive element (IRE) on the promoter activity. Point mutations were introduced into pGL3-IRS2 (–834) to substitute C at nucleotide position to –765 with T [pGL3-IRS2(–765T)] or to disrupt sequence in the insulin-responsive element (IRE) [pGL3-IRS2-mutIRE]. The normalised firefly luciferase activity of Fao cells transfected with pGL3-IRS2(–834) (panel A), pGL3-IRS2 (–765T) (panel B), or pGL3-IRS2-mutIRE (panel C) in the absence or presence of 100 nmol/l insulin was measured and expressed relative to that of pGL3-IRS2(–834) in the absence of insulin. Data are means ± SE of values from six independent experiments and two independent transfections. $*p<0.005$ vs insulin:basal ratio in pGL3-IRS2(–834). **B** EMSA analysis was done with Fao nuclear extract and a ^{32}P-labelled double-stranded oligonucleotide containing C at nt –765 of the *IRS2* promoter (–765C). Competition analysis was done in the presence of –765C (lane 3) or –765T (lane 4) oligonucleotide, respectively. In lane 1, the ^{32}P-labelled probe was applied to the gel without prior incubation with nuclear extract. Shifted bands are indicated with *arrows*. Free, free probe. Data are representative of three similar experiments

Table 4. Comparison of clinical profiles for the –765*C/T* polymorphisms in 5′ UTR of *IRS2* for normal control subjects

	CC	*CT*	*TT*	*p* value[a]	[b]*p*
n (men/women)	59 (27/32)	110 (57/53)	79 (30/49)		
Age (years)	78.0±8.5 (n=59)	74.1±8.0 (n=110)	76.2±8.7 (n=79)	0.011	
Height (cm)	154±9.0 (*n*=58)	156±9.0 (*n*=110)	153±8.7 (*n*=77)	0.081	
Weight (kg)	50.2±9.2 (*n*=58)	52.3±9.8 (*n*=110)	50.0±11.5 (*n*=78)	0.252	
BMI (kg/m²)	21.2± 3.6 (n=58)	21.4±3.2 (n=110)	21.4±4.4 (n=77)	0.950	
HbA$_{1c}$ (%)	5.17±0.31 (n=59)	4.96±0.42 (n=110)	5.08±0.36 (n=79)	0.003	0.006
FPG (mg/dl)	99±19 (n=45)	91±14 (n=81)	93±13 (n=59)	0.027	

[a] *p* values were obtained by one-way ANOVA
[b] *p* values obtained by ANCOVA using age and sex as covariance.

Data are presented in means ± SD
FPG, Fasting plasma glucose

that the two SNPs in the 5′ UTR of *IRS2* were not associated with the susceptibility to Type II diabetes mellitus.

Effect of SNP(–765) and insulin responsive element (IRE) on the transcriptional activity of IRS2 in the presence or absence of insulin. Since the above-identified SNP(–765) was localised in the close proximity of the cis regulatory element (nt –758 to –749) and the HbA$_{1c}$ level was higher in the control subjects with *C/C* than those with *C/T* and *T/T*, it should be possible that this SNP could have an effect on *IRS2* expression. We therefore investigated whether the SNP(–765) affects the transcriptional activity of *IRS2*. *IRS2*-driven reporter activity in the construct bearing thymine at nt –765, pGL3-IRS2(–765T), was approximately ~80% of that of the plasmid containing cytosine at nt –765, pGL3-IRS2(–834), in Fao cells (Fig. 7A) and

HepG2 cells. Because the mRNA expression for *IRS2* was suppressed by the increase in plasma insulin concentration in the *ob/ob* and lipodystrophic mice [27] as well as freshly isolated rat hepatocytes [27, 28], we also examined the effect of insulin on transcriptional activity of these constructs. When measured in Fao cells in the presence of insulin, pGL3-IRS2(–834) showed approximately 50% suppression in *IRS2*-driven reporter activity, compared with that in the absence of insulin (Fig. 7A). In contrast, pGL3-IRS2(–765T) did not show insulin-mediated suppression in *IRS2*-driven reporter activity in Fao cells when compared with its non-stimulated transcriptional activity (Fig. 7A). EMSA analysis indicated that protein-DNA complex visualised by incubation of the ^{32}P-labelled probe containing the partial footprint 1 sequence with Fao nuclear extract was efficiently abolished by the presence of excess unlabelled com-

petitor oligonucleotides containing C at nt –765, whereas those containing T at nt –765 showed only weak competition (Fig. 7B). These results suggested that the SNP(–765T) resulted in the functional alteration on the transcription of *IRS2* by affecting the binding between *IRS*2 and protein(s) required for the transcriptional regulation.

We finally addressed whether the mutation introduced in the so-called "insulin-responsive element (IRE)" (5′-TG<u>TT</u>TTG-3′), identified in our study and elsewhere [28, 29] at nt –570 to –564 of the 5′ UTR of *IRS2*, affects the basal promoter activity and/or insulin-mediated change in the promoter activity (if any) of *IRS2*. Disruption of the IRE heptanucleotide sequence by two-base pairs substitution (–570 5′-TG<u>TT</u>TTG-3′ –565) resulted in a decrease in the *IRS2*-driven reporter activities in the absence of insulin and ablated the insulin-induced suppression in Fao cells (Fig. 7A, panel C).

Discussion

By sequencing the 5′ UTR of human *IRS2* a TATA box was located at nt –2190 to –2184, a location further upstream than that apparent for such elements in most other genes [30]. The transcriptional activity of the plasmid pGL3-IRS2(–2399), which contains the TATA box of *IRS2*, was almost identical to that of pGL3-IRS2(–2116), which lacks the TATA box, suggesting that the human *IRS2* promoter could be functionally TATA-less. The human *IR* [31] and mouse IRS1 [32] genes also seem to lack a typical TATA box as well as a CCAAT box in their 5′ UTRs; these genes have therefore been suggested to function as housekeeping genes [33]. However, with the use of the TFSEARCH program, we identified several CCAAT boxes in the 5′ UTR of human *IRS2*, suggesting that the transcriptional properties of human *IRS2* differ from those of the human *IR* and mouse *IRS1* gene.

We located 10 bp sequence between nt –758 and –749 in the identified footprint 1 region that is suggested to function as cis regulatory element and be involved in the positive regulation of *IRS2*. Supershift analysis showed that polyclonal antibodies to Sp2 or to Sp3 reduced the mobility of the protein-DNA complexes formed by the footprint 1 probe (Fig. 4A, arrowheads); polyclonal antibodies to either AP2, Sp1, Sp4, E2F, gut Krüppel-like factor (GKLF), or HSF had no effect on the migration of these complexes. These results indicated that the supershifted protein-DNA complexes contained Sp2 and Sp3. We suggest however, that the contributions of these two Sp proteins to the promoter activity associated with the footprint 1 region is relatively minor because an oligonucleotide containing the consensus GC box sequence did not compete with the footprint 1 probe in its interaction with nuclear proteins and the binding

of neither the anti-Sp2 nor the anti-Sp3 antibodies resulted in a complete displacement of any of the three bands corresponding to the major DNA-protein complexes. Rather, we consider that the 37 000 M_r protein identified by ultraviolet-induced cross-linking and Southwestern blot analyses potentially binds to this 10-bp sequence, thereby functioning as a major regulatory protein in the transcription of *IRS2*.

Insulin-regulated transcriptional control of *IRS2* was also examined in this study in the context of the recent study describing the involvement of IRE of *IRS2* in the insulin-mediated suppression of *IRS2* transcription [28]. Fao cells transfected with pGL3-IRS2(–765T) did not show a decrease in the basal transcription of *IRS2*-driven reporter, however, preserved a transcriptional activity in the presence of insulin at a level similar with that observed without insulin (Fig. 7A). As a result, this plasmid, pGL3-IRS2(–765T), abolished the insulin-mediated suppression of *IRS2* transcriptional activity. These observations are in contrast with the above-mentioned study as well as our observation in which Fao cells transfected with a human IRS2 containing mutated IRE showed a decrease in the *IRS2*-driven reporter activity in the absence of insulin [28]. We suggest that this latter observation might be a primary reason for the apparent loss of insulin-mediated suppression of *IRS2* transcriptional activity in the cells transfected with *IRS2* containing mutated IRE. In this context, IRE of *IRS2* identified herein and the previous study might not contribute to the ability of IRS2 to mediate signals from insulin to suppress the transcription of *IRS2* itself but would be involved in preserving the basal *IRS2* transcriptional activity. In contrast, the sequence surrounding nt –765 could rather be involved in the pathway which mediate the signals from insulin to suppress *IRS2* transcription in these cells.

The mechanism by which SNP(–765T) altered the insulin-mediated regulation of *IRS2* transcription is currently unclear; however, we showed by EMSA analysis that cytosine residue at nt –765 is indeed involved, whereas thymine residue at the same position is less involved, in the binding between *IRS*2 and protein(s) required for the transcriptional regulation although the sequence surrounding nt –765 (–777 5′-CGGGCCGGGGCCTCCGCGGGAGGGGGA-3′ –751) does not correspond at all with the consensus IRE motif. These results, together with the results of luciferase reporter assay, emphasize the importance of the residue nt –765 in the insulin-mediated transcriptional regulation of *IRS2*.

Given that hyperinsulinaemia leads to a down-regulation of IRS2 in the liver, which is associated with insulin resistance, the ablation of insulin-mediated suppression of IRS2 transcription shown by the SNP(–765T) should have beneficial roles in confronting the glucose tolerance in human subjects with insulin resistance. However, the allele frequencies for this

SNP were not different between the diabetic and the control group. Such favourable effects were neither evident in our experiments comparing many metabolic parameters including BMI and HOMA between Japanese Type II diabetic patients with or without the SNP($-765C/T$). However, results in healthy control subjects, analysed at the same time in this study, could support the hypothesis that T allele at nt -765 have some profitable effects in preserving the normal glucose concentration, as shown by the lower HbA_{1c} in subjects bearing thymine at this position.

In conclusion, we have cloned and sequenced the proximal 2.4-kb of the 5′ flanking region of the human *IRS2* gene, and have identified the sequence, nt -758 to -749, in footprint 1 that contribute to positive regulation of *IRS2* transcription. A 37 000 M_r protein was shown to bind to this 10-bp sequence. We screened the 5′ UTR of human *IRS2* and identified the SNPs ($-765C/T$ and $-2062T/C$). These SNPs were not associated with Type II diabetes, however, the former was suggested to be involved in the insulin-mediated regulation in the transcriptional activity of *IRS2*.

References

1. White MF (1998) The IRS-signaling system: a network of docking proteins that mediate insulin action. Mol Cell Biochem 182:3–11
2. O'Neill T, Craparo A, Gustafson T (1994) Characterization of an interaction between insulin receptor substrate 1 and the insulin receptor by using the two-hybrid system. Mol Cell Biol 14:6433–6442
3. Yenush L, Makati K, Smith-Hall J, Ishibashi O, Myers M, White M (1996) The Pleckstrin Homology domain is the principle link between the insulin receptor and IRS-1. J Biol Chem 271:24300–24306
4. Sawka-Verhelle D, Tartare-Deckert S, White M, Van Obberghen E (1996) Insulin receptor substrate-2 binds to the insulin receptor through its phosphotyrosine binding domain and through a newly identified domain comprising amino acids 591–786. J Biol Chem 271:5980–5983
5. He W, Craparo A, Zhu Y, O'Neill T et al. (1996) Interaction of insulin receptor substrate-2 (IRS2) with the insulin and insulin-like growth factor I receptors. Evidence for two distinct phosphotyrosine-dependent interaction domains within IRS2. J Biol Chem 271:11641–11645
6. Burks DJ, Wang J, Towery H et al. (1998) IRS pleckstrin homology domains bind to acidic motifs in proteins. J Biol Chem 273:31061–31067
7. Tamemoto H, Kadowaki T, Tobe K et al. (1994) Insulin resistance and growth retardation in mice lacking insulin receptor substrate-1. Nature 372:182–186
8. Araki E, Lipes M, Patti M-E et al. (1994) Alternative pathway of insulin signalling in mice with targeted disruption of the IRS-1 gene. Nature 372:186–190
9. Withers D, Gutierrez J, Towery H et al. (1998) Disruption of IRS2 causes type 2 diabetes in mice. Nature 391:900–904
10. Terauchi Y, Iwamoto K, Tamemoto H et al. (1997) Development of non-insulin dependent diabetes mellitus in the double knockout mice with disruption of insulin receptor substrate-1 and beta cell glucokinase genes. Genetic reconstitution of diabetes as a polygenic disease. J Clin Invest 99:861–866
11. Almind K, Bjorbaek C, Vestergaard H, Hansen T, Echwald SM, Pedersen O (1993) Amino acid polymorphisms of insulin receptor substrate–1 in non-insulin-dependent diabetes mellitus. Lancet 342:828–832
12. Mori H, Hashiramoto M, Kishimoto M, Kasuga M (1998) Amino acid polymorphysms of the insulin receptor substrate-1 in Japanese non insulin dependent diabetes mellitus. J Clin Endocrinol Metab 80:2822–2826
13. Sun XJ, Wang LM, Zhang Y (1995) Role of IRS2 in insulin and cytokine signaling. Nature 377:173–177
14. Bernal D, Almind K, Yenush L (1998) IRS2 amino acid polymorphisms are not associated with random type 2 diabetes among Caucasians. Diabetes 47:976–979
15. Almind K, Frederiksen SK, Bernal D (1999) Search for variants of the gene-promoter and the potential phosphotyrosine encoding sequence of the insulin receptor substrate-2 gene: evaluation of their relation with alterations in insulin secretion and insulin sensitivity. Diabetologia 42:1244–1249
16. Mammsrella S, Romano F, Varlerio AD (2000) Interaction between the G1057D variant of IRS-2 and overweight in the pathogenesis of type 2 diabetes. Hum Mol Genet 17:2517–2521
17. Vaßen L, Wegrzyn W, Klein-Hitpass L (1999) Human insulin receptor substrate-2. Gene organization and promoter characterization. Diabetes 48:1877–1880
18. Vaßen L, Wegrzyn W, Klein-Hitpass L (2000) Human insulin receptor substrate-2 is a primary progesterone response gene. Mol Endocrinol 13:485–494
19. Heinemeyer T, Wingender E, Reuter I (1998) Databases on transcriptional regulation: TRANSFAC, TRRD and COMPEL. Nucleic Acids Res 26:362–367
20. Heinemeyer T, Chen X, Karas H et al. (1999) Expanding the TRANSFAC database towards an expert system of regulatory molecular mechanisms. Nucleic Acids Res 27:318–322
21. Schreiber E, Matthias P, Müller MM, Schaffner W (1989) Rapid detection of octamer binding proteins with "miniextracts", prepared from a small number of cells. Nucleic Acids Res 17:6419
22. Laemmli UK (1970) Cleavage of structural proteins during the assembly of the head of bacteriophage T4. Nature 227:680–685
23. Mori H, Ikegami H, Seino S et al. (2000) The Met416→Val variant in the Glycogen Synthase Gene: The prevalence and the association with diabetes in a large number of Japanese individuals. Diabetes Care 23:1709–1710
24. Mori H, Ikegami H, Kawaguchi Y et al. (2001) The Pro12Ala substitution in PPAR-γ is associated with resistance to development of diabetes in the general population: Possible involvement in impairment of insulin secretion in individuals with type 2 diabetes. Diabetes 50:891–894
25. World Health Organization (1985) Diabetes Mellitus: Report of a WHO Study Group. Technical Report Series No 727 World Health Organisation, Geneva

26. Matthews DR, Hosker JP, Rudenski AS, Naylor BA, Treacher DF, Turner RC (1985) Homeostasis model assessment: insulin resistance and β-cell function from fasting plasma glucose and insulin concentration in man. Diabetologia 28:412–419
27. Shimomura I, Matsuda M, Hammer RE, Bashmokov Y, Brown SM, Goldstein JL (2000) Decreased IRS-2 and increased SREBP-1c lead to mixed insulin resisyance and sensitivity in lives of lipodystrophic and ob/ob mice. Mol Cell 6:77–86
28. Zhang J, Ou J, Bashmokov Y, Horton JD, Brown MS, Goldstein JL (2001) Insulin inhibits transcription of IRS-2 gene in rat liver through an insulin response element (IRE) that resembles IREs of other insulin repressed genes. Proc Natl Acad Sci USA 98:3756–3761
29. O'Brien RM, Granner DK (1996) Regulation of gene expression by insulin. Physiol Rev 76:1109–1161
30. Breathnach R, Chambon P (1981) Organization and expression of eucaryotic split genes coding for proteins. Annu Rev Biochem 50:349–383
31. Cameron KE, Resnik J, Webster NJ (1992) Transcriptional regulation of the human insulin receptor promoter. J Biol Chem 267:17375–17383
32. Araki E, Haag BL, Matsuda K, Shichiri M, Kahn CR (1995) Characterization and regulation of the mouse insulin receptor substrate gene promoter. Mol Endocrinol 9:1367–1379
33. Slansky JE, Farnhm PJ (1996) Transcriptional regulation of the dihydrofolate reductase gene. Bioessays 18:55–62